Analysis of Performance Limitations for Superconducting Cavities *

Jean R. Delayen, Lawrence R. Doolittle, and Charles E. Reece
Thomas Jefferson National Accelerator Facility, Newport News, Virginia 23606 USA

Abstract

The performance of superconducting cavities in accelerators can be limited by several factors, such as: field emission, quenches, arcing, rf power; and the maximum gradient at which a cavity can operate will be determined by the lowest of these limitations for that particular cavity. The CEBAF accelerator operates with over 300 cavities and, for each of them, we have determined the maximum operating gradient and its limiting factor. We have developed a model that allows us to determine the distribution of gradients that could be achieved for each of these limitations independently of the others. The result of this analysis can guide an R&D program to achieve the best overall performance improvement. The same model can be used to relate the performance of single-cell and multi-cell cavities.

1 MODEL AND ANALYSIS

We assume n independent random variables X_i, each with probability density $f_i(x)$ and probability distribution $F_i(x) = \int_{-\infty}^{x} f_i(t)dt$.

We define a new random variable X as $X = \min(X_i)$. Its probability density $f(x)$ and distribution $F(x)$ are related to those of the X_i by:

$$1 - F(x) = \prod_i [1 - F_i(x)]$$

$$f(x) = (1 - F(x)) \sum_i \frac{f_i(x)}{1 - F_i(x)}$$

While $f(x)$ and $F(x)$ are directly observable, the above relations are not sufficient to determine the $f_i(x)$ and $F_i(x)$. This can be done, however, if for each realization of X we can identify for which variable X_i we had $x = x_i$.

In the application to superconducting cavities this means that for each cavity, not only do we know the maximum gradient at which it will operate but also which limitation prevents it from operating at a higher field. This is shown in figure 1. For each variable X_i, we can then define the function $g_i(x)$ as:

$$g_i(x)dx = \text{Prob}\{x < X_i \leq x + dx,\ X_j > x \text{ for } j \neq i\}$$

$$= f_i(x)dx \prod_{j \neq i} [1 - F_j(x)]$$

* Work supported by the U.S. DOE Contract # DE-AC05-84ER40150

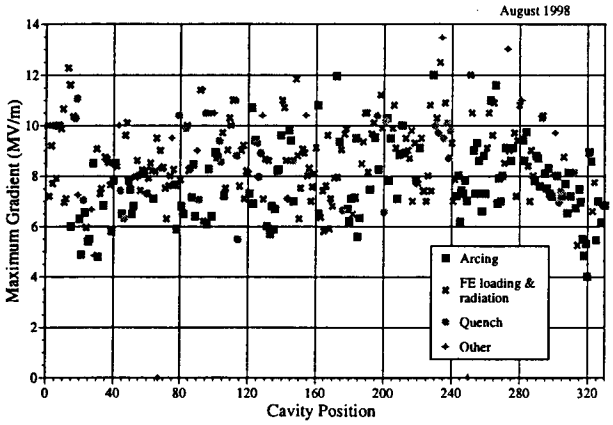

Figure 1: Maximum useful gradient and type of limitation for CEBAF cavities.

$$g_i(x) = \frac{f_i(x)}{1 - F_i(x)} \prod_j [1 - F_j(x)] \qquad (1)$$

The functions $g_i(x)$ are directly observable and the corresponding histograms are shown in figure 2 for our application. Note that the functions $g_i(x)$ are not true probability densities but represent how often a particular variable will be the minimum for a particular value x. The functions $g_i(x)$ also satisfy

$$\sum_i g_i(x) = f(x)$$

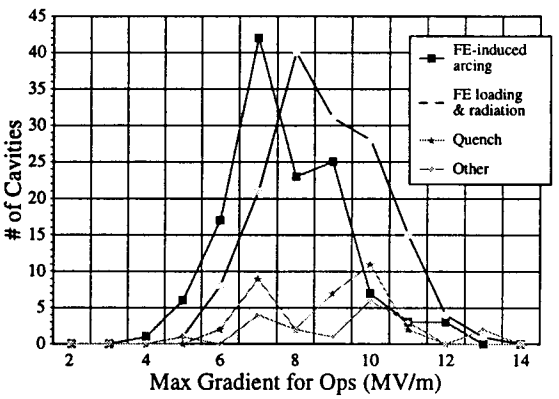

Figure 2: Histograms of the cavity gradients for the different limitations.

Equation (1) can be rewritten as:

$$\frac{f_i(x)}{1 - F_i(x)} = \frac{g_i(x)}{1 - F(x)}$$

Since $f_i(x)$ is the derivative of $F_i(x)$ the above equation can be simply integrated to yield:

$$F_i(x) = 1 - \exp\left(-\int_{-\infty}^{x} \frac{g_i(t)dt}{1-F(t)}\right) \qquad (2)$$

$$f_i(x) = \frac{g_i(x)}{1-F(x)} \exp\left(-\int_{-\infty}^{x} \frac{g_i(t)dt}{1-F(t)}\right)$$

For a finite number of cavities, the measured probability densities $f_i(x)$ are constructed from delta functions. For n cavities, each with a limit of type l_k at energy E_k,

$$g_i(x) = \frac{1}{n}\sum_k \delta(x - E_k)\delta_{i,l_k},$$

where l_k ranges over the same set of integers as i (arcs, radiation, etc.). The distribution F and the individual G_i are easily computed by integration of g_i. As shown in figure 3, they are summations of step-functions.

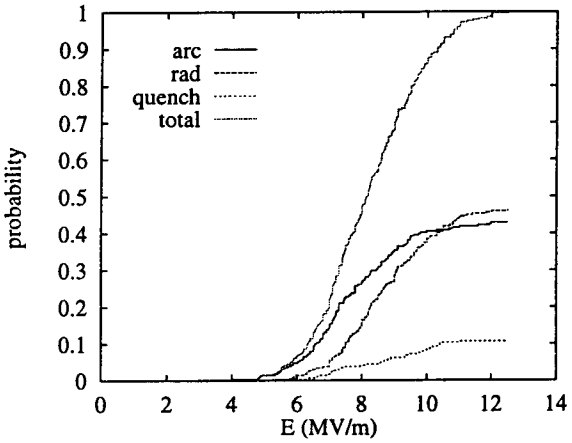

Figure 3: Measured distributions F and G_i vs. energy.

Equation (2) also integrates sums of delta functions into sums of step-functions. The resulting derived probabilities F_i are shown in figure 4, and the corresponding density functions f_i are again sums of delta functions. To be shown in a useful form one could sort them into bins; instead, we assumed they have an approximate log-normal form, and chose coefficients for that distribution based on the calculated F_i.

The smoothed probability densities $f_i(E)$ for the 3 main limitations are shown in figure 5, along with the overall density $f(E)$. The same analysis was performed in 1995 on data collected at that time, and is shown in figure 6.

2 DISCUSSION

Two of the important limitations which were present in 1995 have been eliminated. At that time, the beam current required of the machine was modest, so to reduce power consumption, the output power of the klystrons was limited to 2 kW. This imposed a limit on the gradient that some cavities, whose external Q was not optimal, could achieve. In 1998,

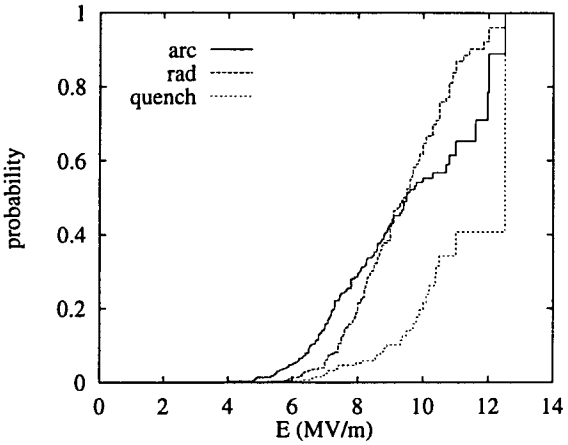

Figure 4: Calculated distributions F_i vs. energy.

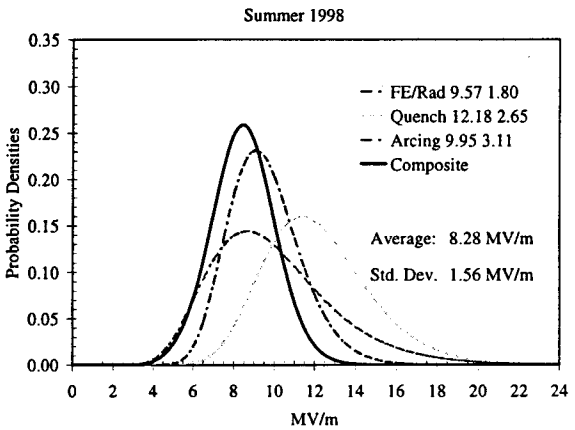

Figure 5: Probability densities for 1998 limitations.

with the klystrons operating at 5 kW output power, rf is not a limitation anymore.

Another limitation which was present in 1995 (labelled WG in the figure) was due to pressure fluctuations in the waveguide section between the cold and warm windows leading to an rf trip. Since then a program to improve *in situ* the performance of the cavities has been implemented. This program includes a cryocycle of the cryomodules to about 40 K to outgas the waveguide section, followed by rf conditioning of the same section. As a result, waveguide pressure fluctuations and their associated rf trips have been eliminated as an important performance limitation [1].

The main limitation, as can be seen from figure 6, was field emission in the cavities. This was the main target of the *in situ* processing of the cavities and, although not yet completed, has resulted in raising the field-emission-limited performance by 1 MV/m. When this improvement program is completed in February 1999 it is expected to have raised the operational energy of CEBAF from 5 to 6 GeV.

As indicated in figure 5 a new limitation has appeared which was not included in the 1995 data. It is due to occasional arcing or flashover on the cold window, which is located close to the beam line, and is probably caused by

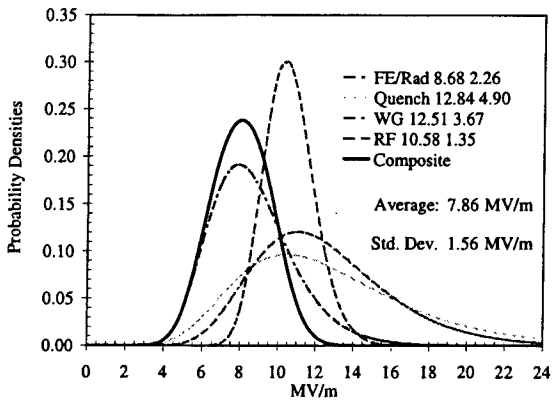

Figure 6: Probability densities for 1995 limitations.

slow charging from field-emitted electrons. This limitation is different from the others in that it is operational in nature, and not as hard a limitation as the others. Although arcing is infrequent (which is why is was not identified in the 1995 commissioning data), with more that 300 cavities in operation it can have a significant impact on accelerator up-time. We have set a limit of less than one arc-related trip every two hours for each of the cavities which display this behavior, and some of these cavities have had their operating gradient reduced as a result.

A new configuration for the cold window, which places it further from the beam line and shields it from field-emitted electrons, has been developed and tested, and has led to a virtual elimination of arcing in laboratory tests. While this modification cannot be done on cryomodules while they are installed in the accelerator, it is being implemented on new cryomodules which are under construction for the FEL, and will be incorporated in the CEBAF cryomodules when the opportunity presents itself.

3 PERFORMANCE OF MULTI-CELL CAVITIES

The same model can be used to predict or compare the performance of cavities composed of different numbers of cells under the same set of assumptions: each individual cell's performance is independent of other's and governed by the same variables, and the performance of a multi-cell cavity is limited by its weaker cell.

If f_1, resp. F_1 are the probability density, resp. distribution for the operating gradient of single-cell cavities and f_n and F_n the same functions for n-cell cavities, then:

$$F_n(E) = 1 - [1 - F_1(E)]^n$$

$$f_n(E) = n f_1(E) [1 - F_1(E)]^{n-1}$$

In particular, if $\langle E_1 \rangle = \int_0^\infty E f_1(E) dE$ and $\langle E_n \rangle = \int_0^\infty E f_n(E) dE$, under reasonable assumptions on $F_1(E)$ one can estimate the reduction in performance $\langle E_n \rangle / \langle E_1 \rangle$ from 1 to n cells. It is found that $\langle E_n \rangle / \langle E_1 \rangle$ is relatively insensitive to the actual shape of $f_1(E)$ but depends strongly, as should be expected, on its normalized standard deviation $\sigma / \langle E_1 \rangle$.

An example is shown in figure 7 where we assumed a log-normal distribution for $f_1(E)$. Figure 8 shows the decrease in average gradient as a function of the number of cells for normalized standard distributions between 0.1 and 0.4. This shows that the expected gradient in multi-cell cavities has a negative power-law dependence on the number of cells. This is similar to the apparent negative power-law dependence on the cavity surface area [2].

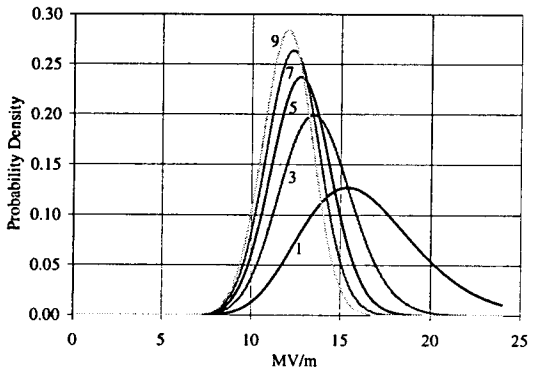

Figure 7: Probability densities for the gradient of single and multi-cell cavities.

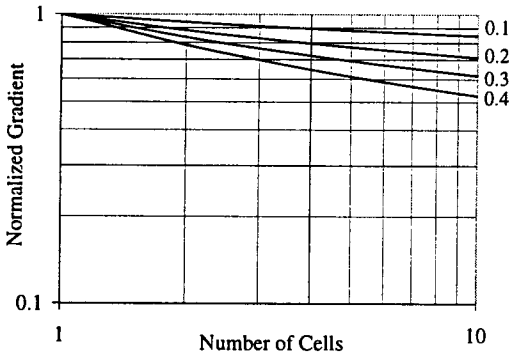

Figure 8: Normalized gradient of multi-cell cavities as a function of the number of cells. The parameter is the normalized standard deviation for gradient of a single-cell cavity.

4 REFERENCES

[1] C. E. Reece *et al.*, "Improvement of the Operational Experience of SRF Cavities via in situ Helium Processing and Waveguide Vacuum Processing," Proc. PAC 95.

[2] H. Padamsee, "Superconducting RF," in AIP Conference Proceedings 249, pp 1402-1482, American Institute of Physics, New York, 1992.